JOC The Journal of Organic Chemistry

Article

pubs.acs.org/joc

Reversible Multistimuli Switching of a Spiropyran-Functionalized Organic Cage in Solid and Solution

Bijnaneswar Mondal, Aloke Kumar Ghosh, and Partha Sarathi Mukherjee*

Inorganic and Physical Chemistry Department, Indian Institute of Science, Bangalore-560012, India

Supporting Information

ABSTRACT: A spiropyran-decorated covalent organic cage (**PC2**) has been designed, employing dynamic imine chemistry followed by imine bond reduction. The molecule is capable of altering its color upon exposure to external stimuli such as heat and light. Construction of a 3D organic cage introduces a new piece to the system by swapping the closed form with the open form in the solid state with diverse color change. Moreover, this material has high chemical stability and is capable of reversible stimuli-responsive color change without any degradation for an extended period.

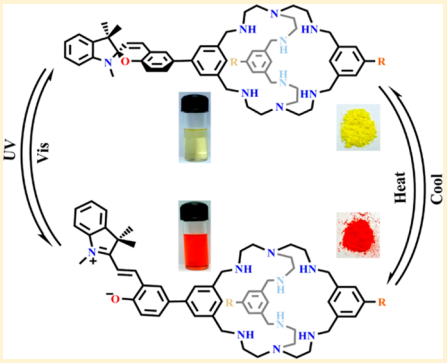

INTRODUCTION

Researchers are fascinated by the materials and systems that can reversibly regulate their structures and properties in reply to environmental stimuli. Stimuli-responsive molecules[1] are capable of changing their structure and/or properties in response to external stimuli such as light, heat, pH, etc. Such molecules have drawn attention as key constituents of stimuli-responsive materials, which include self-darkening windows,[2] self-healing coatings,[3] or silica-based delivery vehicles that can be premeditated to discharge cargo molecules upon activation with a variety of external stimuli.[4] One most common example of a molecular switch is spiropyran (SP), which is hydrophobic and converts into a highly polar open-ring isomer merocyanine (MC) upon exposure to UV light, while the reverse reaction (MC to SP conversion) can be induced by visible light.[5] Moreover, this reversible isomerization can be promoted by a variety of other external stimuli, such as temperature,[6] acids and bases,[7] redox potential,[8] metal ions,[9,10] etc. Among these, light and temperature are two major appealing factors which are environmental friendly in daily use. Due to their tremendous stimuli-responsive nature, spiropyrans have been extensively studied for use in data storage,[11] chemical sensors,[12] smart materials[13,14] etc.

However, the isomerization process requires a large conformational change in the molecule, which is considered to be an unfavorable step in the solid state. To efficiently switch, spiropyran molecules need conformational freedom, which is typically not available within the compactly packed arrays of molecules in the crystalline state. Moreover, as earlier recognized,[15] the metastable MC moieties can stabilize each other by interacting via a combination of electrostatic, dipolar, and $\pi-\pi$ interactions.[16] This stabilization can favor spontaneous SP to MC transition when the closed-ring SP moieties are brought in local proximity.[17] Though solid-state photochromism/thermochromism is more appealing for practical use, simple spiropyran and its derivatives generally show such properties in solution phase mainly. Recently, a few polymers, polyaromatic hydrocarbons, and covalent organic frameworks functionalized with spiropyran have been reported to show such properties in the solid state as well.[18] Negligible solubility of these materials in common solvents limits their fabrication for practical use. So, it is a grand challenge to harvest materials that will be able to show multistimuli responsive character in the solution and solid state with proper longevity.

In the last few decades, discrete three-dimensional (3D) assemblies have commanded extensive attention in various ways, either by their beautifully well-designed architectures or by their significant aptitude to act as sensors,[19] catalysts,[20] and molecular hosts.[21] Nevertheless, dynamic covalent chemistry[22] has appeared as an efficient approach for their easy access, which has been established recently in several cage compounds.[23] A smart way to fulfill the conformational freedom constraint would be to render the spiropyran moieties into a predesigned aldehyde followed by the construction of a 3D architecture. This policy could not only enable efficient isomerization of spiropyran in the solid state but could also help to increase the chemical stability and reversibility using external stimuli (Figure 1).

Herein, we report a spiropyran-functionalized organic amine cage compound **PC2** (Scheme 2) which is soluble in common organic solvents and exhibits multistimuli-responsive properties such as photochromism and thermochromism in both solid and

Received: March 28, 2017
Published: July 5, 2017

DOI: 10.1021/acs.joc.7b00722
J. Org. Chem. 2017, 82, 7783−7790

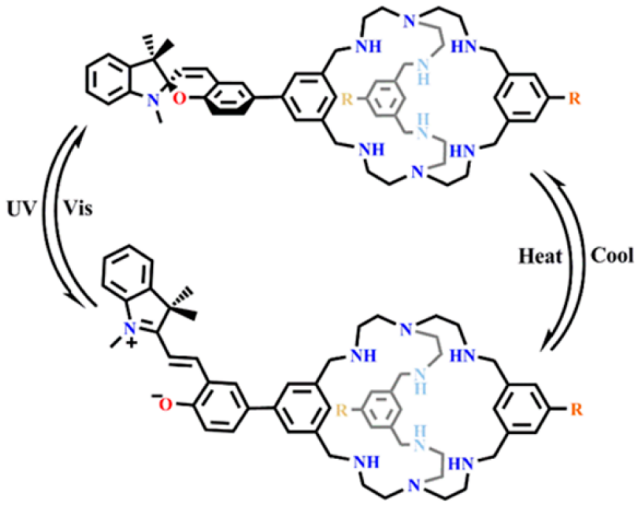

Figure 1. Multistimuli reversible isomerization of the closed form (SP) to open form (MC) in cage **PC2**.

solution state in a reversible manner with superior chemical stability for several cycles.

RESULTS AND DISCUSSION

Synthesis and Characterization of the Cage PC2. Reaction of a spiropyran-functionalized dialdehyde **4** with a flexible triamine tris(2-aminoethyl)amine (tren) easily yielded discrete organic cage **PC2** in 62% yield. The aldehyde building block **4** was synthesized by palladium-catalyzed Suzuki–Miyaura cross-coupling reaction between bromo-spiropyran **3** and diformylphenylboronic ester **2** (Scheme 1). The imine-based cage compound **PC1** was isolated as a yellow solid by treating compound **4** with the triamine "tren" in 3:2 stoichiometric ratio in chloroform at room temperature for 48 h. The cage **PC1** was converted into more stable amine cage **PC2** by sodium borohydride reduction of the dynamic imine bonds. The as-synthesized **PC2** was characterized by multinuclear NMR (^{1}H, ^{13}C), ^{1}H–^{1}H COSY, FT-IR, and ESI-MS analyses. In the ESI-MS spectrum (Figure S23), the peak at m/z = 1425.8788 corresponding to $[M + H]^{+}$ species unequivocally advocates for the formation of the [3 + 2] self-assembled cage. Several efforts to crystallize this cage have so far been unsuccessful.

Scheme 1. Synthetic Route for the Synthesis of Spiropyran-Decorated Dialdehyde 4

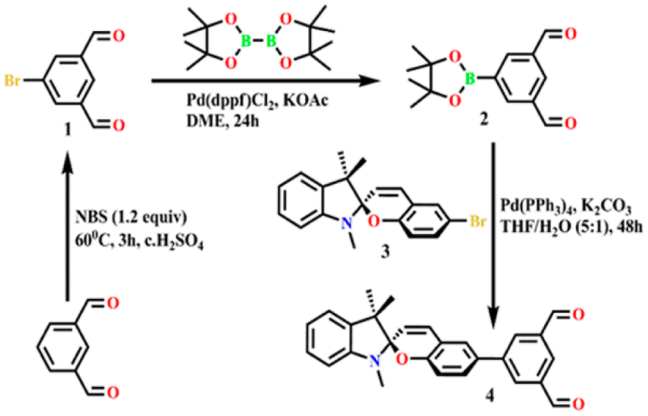

Scheme 2. Synthetic Route for the Synthesis of Organic Cage PC2

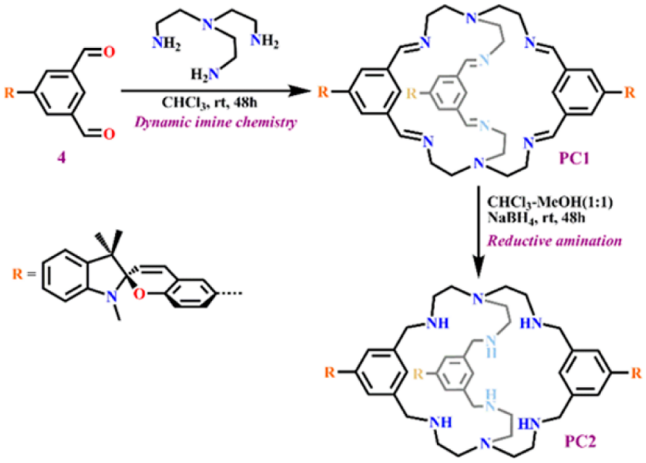

Photochromism and Thermochromism in the Solution State. Compounds containing spiropyran moieties are well-known for their photochromic and thermochromic behavior. Therefore, organic cage **PC2** decorated with spiropyran in its aromatic backbone shows SP–MC isomerization which can be triggered by UV light and heat.

As can be seen from the UV–vis absorption of **PC2** in Figure 2, the compound can undergo reversible photoisomerization between their closed-isomer SP and open-isomer SP under a UV lamp. The absorption peak at 293 nm for the closed form of **PC2** decreased, and new absorption peaks at 520 and 552 nm assigned to the open form appeared and increased with increased duration of exposure time.

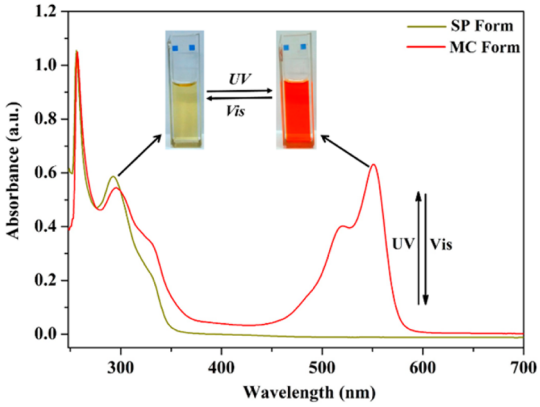

Figure 2. UV–vis absorption spectra of cage **PC2** (2 mL, 10^{-5} M) in dimethyl sulfoxide recorded under ultraviolet irradiation. The inset shows digital photographs of SP and MC forms of cage **PC2** in the solution state.

In the reverse phenomenon, the peak intensity of the open isomer was gradually decreased over a time period of 2 h under visible light (Figure 3). In view of this fact, the excitation at 520 and 552 nm shows the same pattern in the fluorescence spectra, suggesting that it is due to the MC isomer of the cage (Figure S24). Moreover, a similar thermochromic behavior is also perceived for cage **PC2** in UV–vis and fluorescence spectroscopy (Figures S25 and S26), and the reversible phenomenon (MC form transforms to SP form) takes place by cooling to room temperature with gradual decoloration (Figure S27).

DOI: 10.1021/acs.joc.7b00722
J. Org. Chem. 2017, 82, 7783–7790

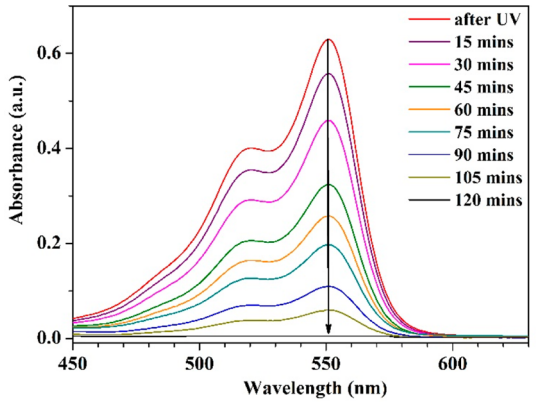

Figure 3. Change in absorption spectra of the MC form of the cage **PC2** (2 mL, 10^{-5} M) in dimethyl sulfoxide upon exposure to visible light.

Photochromism and Thermochromism in the Solid State. As discussed earlier, color change due to structural isomerization of stimuli-responsive materials in their solid state is really challenging for practical applications. Simple spiropyran derivatives generally do not show such structural isomerization in the solid state. Similarly, the spiropyran precursor molecules **3** and **4** did not undergo any isomerization in the solid state upon exposure to UV radiation or heating (Figures S32–S37). Interestingly, the reduced amine cage **PC2** was able to show both photoisomerization and thermoisomerization with a distinct color change in the solid state. The bright yellow color of the SP form of the cage gradually turns to the red MC form upon exposure to a UV lamp over a time period of 2.5 h (Figure 4). The reversible phenomenon was observed upon

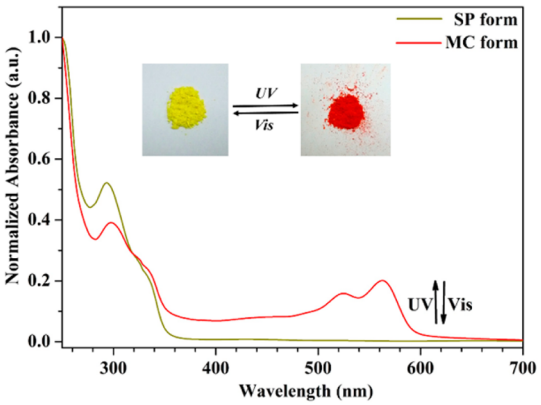

Figure 4. UV–vis absorption spectra of a thin film of **PC2** recorded under ultraviolet irradiation. The inset shows digital photographs of SP and MC forms of the cage **PC2** in the solid state.

exposure to visible light with gradual decoloration within 2 h (Figure 5). Similarly, solid powder of **PC2** was heated at 80 °C for 2.5 h which converts the yellow closed form (SP analogue) to the red open form (MC analogue) (Figures S29 and S30).

As can be seen from the solid-state UV–vis absorption spectrum of **PC2** in Figure 4, the absorption peak intensity at 293 nm for the SP form of **PC2** decreased and new absorption peaks at 525 and 563 nm assigned to the open form appeared upon exposure to UV light. In the reverse phenomenon, the peak intensity of the open isomer was gradually decreased over a time period of 2 h under visible light (Figure 5). In view of

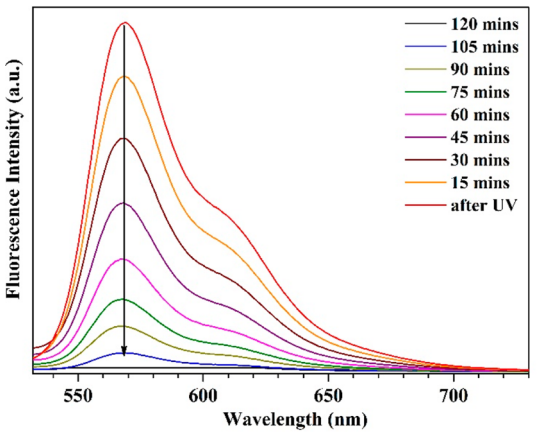

Figure 5. Change in emission spectra of a thin film of cage **PC2** (MC analogue) upon exposure to visible light.

this fact, the excitation at 525 and 563 nm shows a similar pattern in fluorescence spectra, suggesting that the MC isomer of the cage is formed (Figure S28). Moreover, a similar thermochromic behavior was also observed for **PC2** in UV–vis and fluorescence spectroscopy (Figures S29 and S30), and the reversible phenomenon took place by cooling to room temperature over a time period of 2 h (Figure S31). On acidification, the red MC isomer transformed to its protonated MCH^+ form which showed a characteristic band[5j] around 430 nm in UV–vis spectrum (Figures S51 and S52). Moreover, the MCH^+ isomer was quite stable for long period under visible light in the solid state (Figure S53). Similarly, MC to MCH^+ transformation was also observed in heating–cooling cycle upon acidification, and the protonated form was intact for a long time at room temperature (Figures S54–S56).

The precursor compounds **3** and **4** are not able to show isomerization presumably due to the lack of conformational freedom in compactly crammed arrays of molecules which did not allow the closed-form to open-form transformation in the solid state.

Moreover, the chemical stability of compounds **3** and **4** is relatively low under UV radiation or heating for several hours in the solid state which is reflected in their UV–vis spectra (Figures S32, S34, S35, and S37) whereas in the 3D organic cage architecture (**PC2**), there is enough space for conformational changes. Moreover, very close/dense packing of the larger cage molecules is unlikely due to steric crowding in the solid state. Such arrangement of the cage molecules in the solid state may lead to loosely packed arrays of molecules with enough intermolecular space for isomerization of the SP moiety to the MC moiety or vice versa to show reversible photochromism and thermochromism.

Morphology and Crystallinity in the Solid State. Scanning electron microscopy (SEM) images were taken to investigate the surface morphology of the cage **PC2** in both closed and open forms. "Long rod-shape" microstructures were perceived in the SP form of cage **PC2** whereas "random edged" microstructures were observed in its open form upon exposure to UV radiation or heat for several hours (Figure 6). A reversible phenomenon is noticed upon the removal of external stimuli where "random edged" microparticles are converted into "long rod-shape" microparticles. Fortunately, we were also able to get such intermediate images where both kinds of microstructures were present in a time-dependent experiment (Figures S47–S49).

DOI: 10.1021/acs.joc.7b00722
J. Org. Chem. 2017, 82, 7783–7790

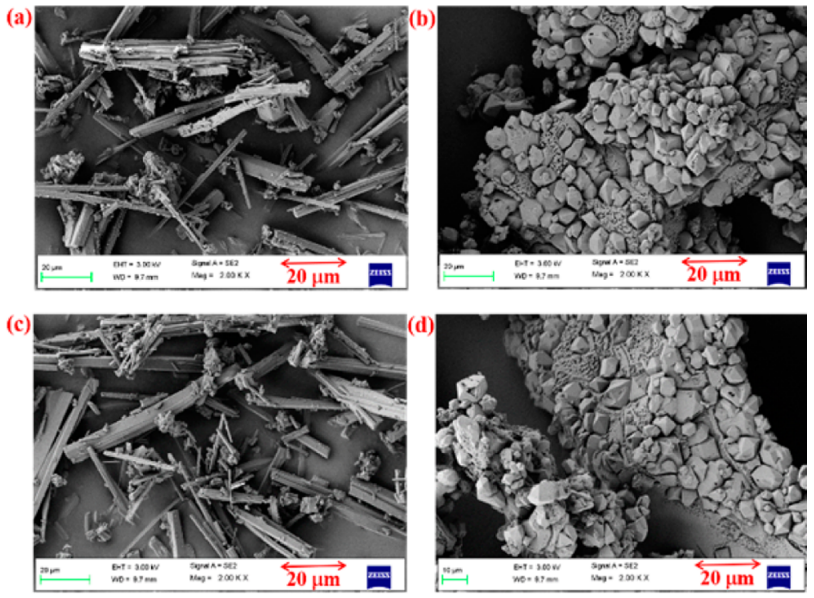

Figure 6. SEM images of cage **PC2** (a) before (b) after UV radiation and (c) before (d) after heating.

PXRD data were collected to check the crystalline nature of the material in both SP and MC states. A highly crystalline pattern was observed in PXRD analysis for the SP analogue which was also suggested by the SEM images. We performed a short (30 min) PXRD analysis for the MC state, as it is reversible in visible light and ambient temperature. Though the scan time period is short, we observed a crystalline pattern which is quite different from that of the SP state. After one complete UV–vis cycle, the material showed a PXRD pattern identical to that of the as-synthesized material (Figure 7) due to

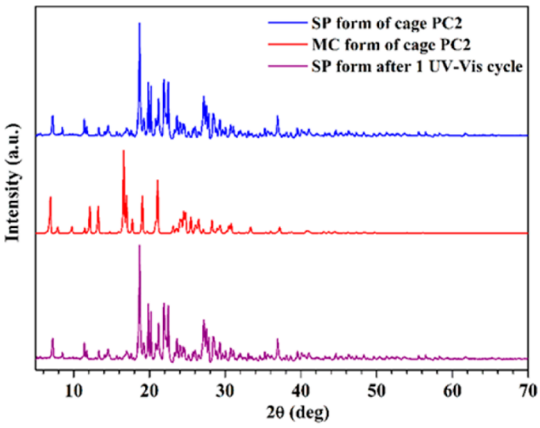

Figure 7. PXRD patterns of cage **PC2** in the SP form (blue line), in the MC form (red line), and after one UV–vis cycle (purple line).

the reversible nature of the SP–MC forms of the cage **PC2**. In the DSC thermogram, the appearance of two small sharp peaks around 80 °C suggests that **PC2** undergoes phase transition (Figure S50). This result implies that **PC2** reversibly converts between two disparate solid-state microstructures via a phase transition induced by external stimuli.

Reversibility in the Solution and Solid State. Reversibility is the crucial factor for practical application of any fatigue-free molecular switch with multistimuli-responsive nature which makes it more beneficial for its industrial and scientific applications. Moreover, the existence of chemical stability is a vital point for protecting the photochromic dye from environmental deprivation and induces proper longevity. Hence, to address the concern for this material (**PC2**), both the solution and solid states were tested for the SP to MC form and vice versa for up to at least 20 consecutive cycles. As portrayed in Figure 8a (Figure S39), experimental results indicate a negligible amount of decrease in absorbance in the solution state. Similar behavior was also observed in the solid-state UV–vis spectra for at least 20 UV–vis consecutive cycles (Figures 8c and S43). Both solution- and solid-state UV–vis studies were carried out to check its reversible nature for at least 20 consecutive heating–cooling cycles (Figures S40, S41, S44, and S45). It was found that the absorbance peak of the MC form of cage **PC2** at 550 and 563 nm for the solution and solid states, respectively, showed no considerable change in intensity.

The SEM images of the solid **PC2** after 20 cycles also suggested no significant change in the size and morphology of this material (Figure 9). Also to check its reversibility as well as crystallinity in the solid state, PXRD analysis of the SP form of cage **PC2** was carried out before and after 20 consecutive UV–vis and heating–cooling cycles (Figure S46). These results further supported the fact that the material retains high chemical stability under several UV–vis cycles and heating–cooling cycles without any depreciation for an extended period.

CONCLUSION

In summary, we report here a new discrete organic cage compound having spiropyran moieties in its exterior aromatic backbone. The compound shows reversible thermochromism and photochromism. This newly synthesized cage represents a rare example of a multistimuli-responsive reversible molecular switch in both solution and solid states. Photochromism of the compound involves a ring-closed to ring-open transformation of the spiropyran moiety. Moreover, this cage compound is sensitive to temperature and shows a reversible distinct color change upon heating and cooling. These outcomes represent the first demonstration of the use of a discrete organic cage as a unique model for photochromism and thermochromism in the solid state. The simple spiropyran precursor unit does not show any photochromism/thermochromism in the solid state, while

DOI: 10.1021/acs.joc.7b00722
J. Org. Chem. 2017, 82, 7783–7790

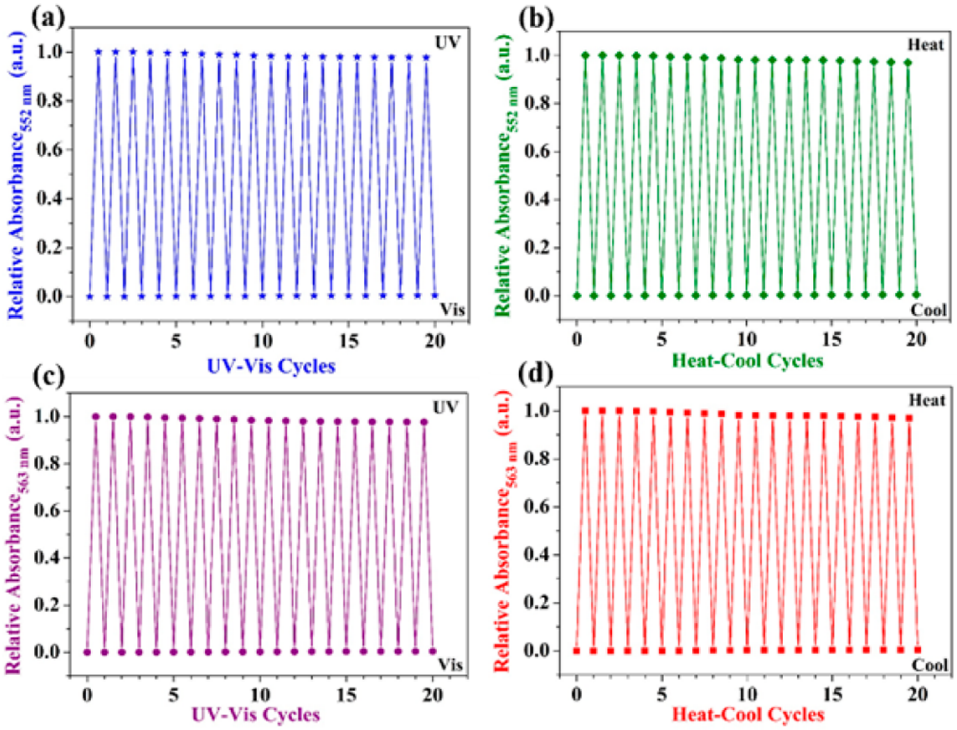

Figure 8. Reversibility of cage **PC2** in the solution state upon (a) UV−vis cycles and (b) heating−cooling cycles and in the solid state upon (c) UV−vis cycles and (d) heating−cooling cycles.

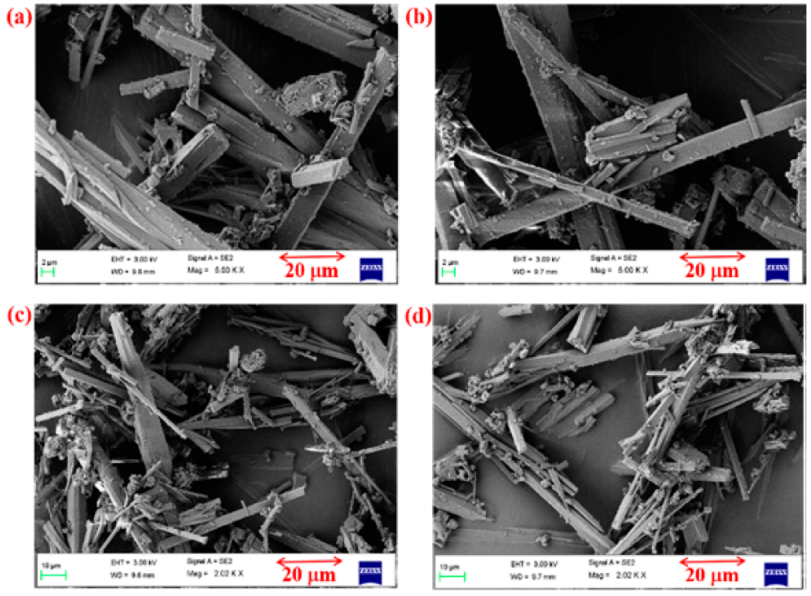

Figure 9. SEM images of cage **PC2** (a) before (b) after 20 UV−vis cycles and (c) before (d) after 20 heating−cooling cycles.

the attachment of this spiropyran unit to a covalent cage leads to conformational isomerization with distinct color change in the solid state. Reversibility and chemical stability of this cage compound are well retained even after 20 cycles. The material is noteworthy, as it does not produce any photofatigued side products and is soluble in common organic solvents. Furthermore, the surface morphology and crystalline patterns have been properly investigated for both the closed and open forms. The present strategy of functionalization of a covalent cage with proper functional groups for the generation of a solid-state stimuli-responsive molecular switch has the potential to develop a new generation of optical switches for practical use.

EXPERIMENTAL SECTION

Materials and Methods. All the chemicals and solvents used for synthesis were purchased from different commercial sources and were not purified further. The NMR spectra were recorded on a Bruker 400 MHz instrument. The chemical shifts (δ) in the ^{1}H and ^{13}C NMR spectra are reported in ppm relative to tetramethylsilane (Me_4Si) as an internal standard (0.0 ppm) in $CDCl_3$. High-resolution mass spectra were recorded on a Q-TOF instrument by an electrospray ionization (ESI) technique using standard spectroscopic-grade solvents. FTIR

DOI: 10.1021/acs.joc.7b00722
J. Org. Chem. 2017, 82, 7783−7790

spectra were recorded on a Bruker ALPHA FTIR spectrometer. Powder X-ray diffraction (PXRD) patterns were recorded on a Phillips PANalytical diffractometer. Scanning electron microscopy (SEM) was performed on a Carl-Zeiss Ultra 55 at an operating voltage of 3−5 kV. Electronic absorption and emission spectra were recorded using a PerkinElmer LAMBDA 750 UV−visible spectrophotometer and a HORIBA Jobin Yvon Fluoromax-4 spectrometer, respectively. A PerkinElmer LAMBDA 35 spectrometer and HORIBA Jobin Yvon Fluorolog4 spectrometer were used to record solid-state UV−vis spectra and fluorescence spectra, respectively. A Powerstar HQI-BT 400W/D E40 lamp was used for UV radiation with low-temperature equipment, and the visible light source was a common 75 W LED lamp with white light. An Analab μ-ThermoCal10 instrument was used for melting point range determination. Thermal characterization was carried out using a PerkinElmer DSC instrument at a heating rate of 1 °C/min under a dry nitrogen atmosphere. Elemental analyses (C, H, N) were carried out in a PerkinElmer 240C elemental analyzer.

Synthesis of ***1***. Compound **1** was prepared according to the literature procedure.[24] ^{1}H NMR ($CDCl_3$, 400 MHz): δ 10.06 (s, 2H), 8.30 (t, J = 1.5 Hz, 1H), 8.26 (d, J = 1.5 Hz, 2H). ^{13}C NMR ($CDCl_3$, 100 MHz): δ 189.6, 138.5, 137.2, 129.3, 124.4. FTIR (cm^{-1}): ν 1685 (C═O).

Synthesis of ***2***. Compound **1** (1 g, 4.7 mmol), bis(pinacolato)-diboron (2.384 g, 9.38 mmol), KOAc (7.370 g, 75.2 mmol), and $Pd(dppf)Cl_2$ (192 mg, 5 mol %) were charged with 60 mL of dry 1,2-dimethoxyethane (DME) in a two-neck flask under nitrogen atmosphere. The reaction mixture was degassed and refluxed with stirring under nitrogen atmosphere for 24 h. The reaction was cooled to room temperature and dried under vacuum and extracted with $CHCl_3$ (20 mL × 3). The combined organic phase was washed with brine solution (20 mL × 3) and dried with anhydrous Na_2SO_4. The filtered organic solvent was dried over reduced pressure, and the residue was purified by the column chromatography using silica gel and hexane to obtain white compound **2**. Isolated yield: 85% (1039 mg, 4 mmol). Melting point range: (102−104 °C); ^{1}H NMR ($CDCl_3$, 400 MHz): δ 10.12 (s, 2H), 8.55 (d, J = 1.5 Hz, 2H), 8.45 (t, J = 1.5 Hz, 1H), 1.37 (s, 12H). ^{13}C NMR ($CDCl_3$, 100 MHz): δ 191.4, 141.4, 136.4, 132.2, 84.8, 24.9. HRMS (ESI-TOF) m/z: $[M + H]^+$ Calcd for $C_{14}H_{17}BO_4$ 261.1298; found 261.1292. FTIR (cm^{-1}): ν 1689 (C═O).

Synthesis of ***3***. Compound **3** was prepared according to the literature procedure.[25] ^{1}H NMR ($CDCl_3$, 400 MHz): δ 7.21−7.16 (m, 3H), 7.08 (d, J = 7.3 Hz, 1H), 6.87 (t, J = 7.3 Hz, 1H), 6.79 (d, J = 10.3 Hz, 1H), 6.60 (d, J = 9.3 Hz, 1H), 6.54 (d, J = 7.6 Hz, 1H), 5.74 (d, J = 10.3 Hz, 1H), 2.72 (s, 3H), 1.30 (s, 3H), 1.17 (s, 3H). ^{13}C NMR ($CDCl_3$, 100 MHz): δ 153.6, 148.1, 136.6, 132.3, 129.2, 128.5, 127.8, 121.6, 120.8, 119.4, 116.9, 111.9, 106.9, 104.6, 52.0, 29.0, 25.9, 20.2. HRMS (ESI-TOF) m/z: $[M + H]^+$ Calcd for $C_{19}H_{18}NOBr$ 356.0650; found 356.0635.

Synthesis of ***4***. In a 250 mL double-neck round-bottom flask, 355 mg (1 mmol) of compound **2** and 390 mg (1.5 mmol) of compound **3** were taken in 100 mL of THF and into that 20 mL of aqueous solution of 414 mg (3 mmol) of K_2CO_3 was added. The resulting mixture was degassed under nitrogen atmosphere. Then it was cooled to room temperature followed by addition of 70 mg (5 mol %) of $Pd(PPh_3)_4$ and heated at 70 °C for 48 h. After the reaction was completed, the mixture was concentrated under high vacuum and extracted with $CHCl_3$. The organic phase was dried over anhydrous Na_2SO_4, and the filtered organic phase was dried under reduced pressure. The crude product was purified by preparative TLC plates using silica gel as stationary phase and chloroform as eluent to get a bright yellow powder of **4**. Isolated yield: 54% (221 mg, 0.54 mmol). Melting point range: (114−116 °C); ^{1}H NMR ($CDCl_3$, 400 MHz): δ 10.04 (s, 2H), 8.29 (s, 1H), 8.25 (s, 2H), 7.18−7.13 (m, 3H), 7.06 (d, J = 7.3 Hz, 1H), 6.84 (t, J = 7.3 Hz, 1H), 6.78 (d, J = 10.3 Hz, 1H), 6.58 (d, J = 9.3 Hz, 1H), 6.52 (d, J = 7.6 Hz, 1H), 5.74 (d, J = 10.3 Hz, 1H), 2.71 (s, 3H), 1.29 (s, 3H), 1.15 (s, 3H). ^{13}C NMR ($CDCl_3$, 100 MHz): δ 189.6, 153.6, 148.1, 138.5, 137.2, 136.6, 132.3, 129.3, 129.1, 128.4, 127.7, 124.4, 121.6, 120.8, 119.4, 116.9, 111.8, 106.9, 104.6, 51.9, 28.9, 25.9, 20.2. HRMS (ESI-TOF) m/z: $[M + H]^+$ Calcd for $C_{27}H_{23}NO_3$ 410.1756; found 410.1757. FTIR (cm^{-1}): ν 1606 (C═O).

Synthesis of ***PC1***. In a 250 mL round-bottom flask, 50 mL of $CHCl_3$ solution of tris(2-aminoethyl)amine (24 mg, 0.16 mmol) was added slowly to a stirring solution of aldehyde **4** (100 mg, 0.24 mmol) dissolved in 100 mL of $CHCl_3$. The resulting reaction mixture was stirred at room temperature for 48 h. After completion of the reaction, solvent was removed and the obtained deep yellow solid was washed with CH_3OH several times. Isolated yield: 68% (78 mg, 0.05 mmol). Melting point range: (124−126 °C); ^{1}H NMR ($CDCl_3$, 400 MHz): δ 8.34 (s, 6H), 7.54 (s, 6H), 7.21−7.16 (m, 9H), 7.08 (d, J = 7.3 Hz, 3H), 6.86 (t, J = 7.3 Hz, 3H), 6.79 (d, J = 10.3 Hz, 3H), 6.60 (d, J = 9.4 Hz, 3H), 6.53 (d, J = 7.6 Hz, 3H), 5.73 (d, J = 10.3 Hz, 3H), 5.41 (s, 3H), 3.79−3.32 (br d, 12H), 2.94−2.72 (br d, 12H), 2.72 (s, 9H), 1.30 (s, 9H), 1.17 (s, 9H). ^{13}C NMR ($CDCl_3$, 100 MHz): δ 158.9, 153.6, 148.1, 138.8, 136.6, 132.3, 130.1, 129.1, 128.5, 127.8, 124.1, 121.6, 120.8, 120.7, 119.4, 116.9, 111.8, 106.9, 104.6, 59.9, 55.7, 51.9, 29.0, 25.9, 20.2. HRMS (ESI-TOF) m/z: $[M + H]^+$ Calcd for $C_{93}H_{93}N_{11}O_3$ 1413.7575; found 1413.7582, $[M + 2H]^{2+}$ Calcd 707.3826; found 707.3844. FTIR (cm^{-1}): ν 2871, 2808, 1641 (CH = N), 1563, 1429, 1333, 1292, 1254, 1155, 1066, 1029, 921, 883, 804, 744, 675, 558.

Synthesis of ***PC2***. A 180 mg (0.12 mmol) amount of **PC1** was taken up in 150 mL of $CHCl_3$−MeOH (1:1, v/v) binary solvent mixture in a 250 mL round-bottom flask. Into this reaction mixture, 58 mg (1.53 mmol) of $NaBH_4$ was added portionwise at room temperature and stirred for 48 h. After completion of the reaction, the solvent was completely removed and the product was extracted in $CHCl_3$. The organic part was washed several times with water and dried over Na_2SO_4 followed by removal of solvent to get a pale yellow solid. Isolated yield: 62% (112 mg, 0.07 mmol). Melting point range: (126−127 °C); ^{1}H NMR ($CDCl_3$, 400 MHz): δ 7.40 (s, 6H), 7.19−7.15 (m, 9H), 7.06 (d, J = 7.2 Hz, 3H), 6.85 (s, 3H), 6.83 (t, J = 7.3 Hz, 3H), 6.78 (d, J = 10.3 Hz, 3H), 6.59 (d, J = 9.3 Hz, 3H), 6.52 (d, J = 7.6 Hz, 3H), 5.72 (d, J = 10.3 Hz, 3H), 3.56 (s, 12H), 2.71 (s, 9H), 2.63−2.62 (d, J = 5.1 Hz, 24H), 1.29 (s, 9H), 1.15 (s, 9H). ^{13}C NMR ($CDCl_3$, 100 MHz): δ 153.6, 148.1, 143.1, 136.6, 132.3, 129.0, 128.4, 127.7, 125.5, 122.5, 121.6, 120.8, 120.7, 119.4, 116.9, 111.8, 106.9, 104.6, 55.4, 53.2, 51.9, 47.9, 28.9, 25.9, 20.2. HRMS (ESI-TOF) m/z: $[M + H]^+$ Calcd for $C_{93}H_{105}N_{11}O_3$ 1425.8514; found 1425.8525. FTIR (cm^{-1}): ν 3296, 2813, 1568, 1442, 1324, 1198, 1131, 1050, 983, 922, 867, 818, 780, 680, 635. Anal. Calcd for $C_{93}H_{105}N_{11}O_3$: C, 78.39; H, 7.43; N, 10.81. Found: C, 78.41; H, 7.41; N, 10.84.

Sample Preparation for Solution-State UV−vis and Fluorescence Spectroscopy. To prepare a 10^{-3} (M) stock solution, 14.24 mg of **PC2** was added to a 10 mL of DMSO and stirred for a few minutes to obtain a clear yellow solution (SP form) at room temperature. In a quartz cuvette, 1980 μL of DMSO and 20 μL of stock solution was added to get a 2 mL of a 10^{-5} M solution. This solution was used for UV−vis spectrum analysis. Then it was irradiated for 2 h with UV light to get a red solution (MC form), and the UV−vis spectrum was measured immediately. This method was repeated to check reversibility for up to 20 UV−vis cycles. The same method was repeated for the heating−cooling cycle and to check reversibility for 20 cycles. For recording the fluorescence spectrum, the same method was used for making a 10^{-5} M solution of **PC2** in DMSO. Then the emission spectra of the MC form of **PC2** were recorded by excitation at 520 and 552 nm.

Sample Preparation for Solid-State UV−vis and Fluorescence Spectroscopy. In a typical stock solution preparation, 20 mg of **PC2** was dissolved in 2 mL of DMSO. A few drops of this solution was placed on a clean quartz plate to make an ultrathin film by a spin-coating method. This thin film was used to measure the solid-state UV−vis spectrum. Then it was irradiated for 2.5 h with UV light, and again the UV−vis spectrum was recorded immediately. This thin film was used to check reversibility for up to 20 UV−vis cycles. The same method was repeated for heating−cooling and used for 20 cycles to check reversibility. For the fluorescence spectrum, the same method was used for making a thin film of **PC2** on a quartz plate. Then emission spectra of the MC form of cage **PC2** were recorded by excitation at 525 and 563 nm.

DOI: 10.1021/acs.joc.7b00722
J. Org. Chem. 2017, 82, 7783−7790

Sample Preparation for Solid-State UV−vis Spectroscopy upon Acidification. In a typical stock solution preparation, 14.2 mg of **PC2** was dissolved in 1 mL of DMSO. This solution was coated on a clean quartz plate to make a thin film by a spin-coating method. This thin film (**PC2**-SP) was used to record it is the solid state UV−vis spectrum. Then it was irradiated for 2.5 h with UV light, and again the UV−vis spectrum was recorded immediately (**PC2**-MC). Ten equivalents of HCl was added on this, and the color changed from red to pinkish (**PC2**-MCH$^+$). Then again the UV−vis spectrum was recorded. After keeping this plate under visible light for 6 h, UV−vis spectrum was recorded. The same method was followed during the heating−cooling cycle upon acidification.

Sample Preparation for Scanning Electron Microscopy (SEM) Analysis. Yellow (SP form) solid sample (1 mg) was placed on a carbon tape, and SEM analysis was performed. Red colored (MC form) solid sample (1 mg) was placed on a carbon tape immediately after the UV radiation, and then SEM analysis was performed to check the morphology. To check reversibility, after 20 consecutive UV−vis cycles, the yellow colored (SP form) material was placed on carbon tape and SEM analysis was carried out. The same method was followed for heating−cooling cycles to check the reversibility. To get intermediate images, first the SP form was converted to the MC form by UV radiation; then this material was placed under visible light for 20 min and immediately placed on a carbon tape for SEM analysis. For the heating−cooling cycle, the same procedure was followed where it was kept for 20 min at room temperature. All the SEM analyses were carried out at 22 °C which does not have that much effect on the conversion time of the MC to SP form.

Sample Preparation for PXRD Analysis. As-synthesized yellow (SP form) cage **PC2** was placed on a flat silicon plate, and PXRD was carried out. This material was irradiated with UV light to convert it into the MC form (red color), and immediately PXRD was carried out for 30 min. After attaining the SP form, the same material was again used for PXRD analysis to check crystallinity. To check its chemical stability and crystallinity after 20 consecutive UV−vis and heating−cooling cycles, the material was used for PXRD analysis. Then it was compared with PXRD patterns of as-synthesized material.

■ ASSOCIATED CONTENT

Supporting Information

The Supporting Information is available free of charge on the ACS Publications website at DOI: 10.1021/acs.joc.7b00722.

^{1}H, ^{13}C, and ^{1}H−^{1}H COSY NMR of the compounds, PXRD, SEM, and ESI-MS, FTIR, UV−vis, and fluorescence spectra of the cage compound (PDF)

■ AUTHOR INFORMATION

Corresponding Author

*E-mail: psm@ipc.iisc.ernet.in.

ORCID

Partha Sarathi Mukherjee: 0000-0001-6891-6697

Notes

The authors declare no competing financial interest.

■ ACKNOWLEDGMENTS

P.S.M. is grateful to DST-New Delhi (India) for Swarnajayanti Fellowship (DST/SJF/CSA-01/2011-12). B.M. acknowledges the CSIR (New Delhi) for research fellowship. A.K.G. is grateful to UGC (India) for Dr. D. S. Kothari Postdoctoral fellowship. We are thankful to Mr. Abhisek Mahapatra for solid-state UV−vis and fluorescence spectral analysis and Mr. Rupak Saha for PXRD data collection. We are also thankful to Ms. Saheli Chakrabarty for DSC experiment.

■ REFERENCES

(1) Feringa, B. L.; Browne, W. R. *Molecular Switches*; Wiley-VCH: New York, 2011.

(2) McCarthy, W. R.; Powers, M. US Patent 20110102878 A1, 2011.

(3) (a) Burnworth, M.; Tang, L.; Kumpfer, J. R.; Duncan, A. J.; Beyer, F. L.; Fiore, G. L.; Rowan, S. J.; Weder, C. *Nature* **2011**, *472*, 334−337. (b) Ito, K. *Curr. Opin. Solid State Mater. Sci.* **2010**, *14*, 28−34. (c) Ito, K.; Araki, J.; Suzuki, T.; Yamanaka, M.; Watanabe, K. US Patent 7943718 B2, 2011.

(4) (a) Cotí, K. K.; Belowich, M. E.; Liong, M.; Ambrogio, M. W.; Lau, Y. A.; Khatib, H. A.; Zink, J. I.; Khashab, N. M.; Stoddart, J. F. *Nanoscale* **2009**, *1*, 16−39. (b) Li, Z. X.; Barnes, J. C.; Bosoy, A.; Stoddart, J. F.; Zink, J. I. *Chem. Soc. Rev.* **2012**, *41*, 2590−2605.

(5) (a) Berkovic, G.; Krongauz, V.; Weiss, V. *Chem. Rev.* **2000**, *100*, 1741−1753. (b) Minkin, V. I. *Chem. Rev.* **2004**, *104*, 2751−2776. (c) Andersson, J.; Li, S.; Lincoln, P.; Andreasson, J. *J. Am. Chem. Soc.* **2008**, *130*, 11836−11837. (d) Buback, J.; Kullmann, M.; Langhojer, F.; Nuernberger, P.; Schmidt, R.; Wurthner, F.; Brixner, T. *J. Am. Chem. Soc.* **2010**, *132*, 16510−16519. (e) Chovnik, O.; Balgley, R.; Goldman, J. R.; Klajn, R. *J. Am. Chem. Soc.* **2012**, *134*, 19564−19567. (f) Klajn, R.; Bishop, K. J.; Fialkowski, M.; Paszewski, M.; Campbell, C. J.; Gray, T. P.; Grzybowski, B. A. *Science* **2007**, *316*, 261−264. (g) Maity, C.; Hendriksen, W. E.; van Esch, J. H.; Eelkema, R. *Angew. Chem., Int. Ed.* **2015**, *54*, 998−1001. (h) Liu, Z.; Liu, T.; Lin, Q.; Bao, C.; Zhu, L. *Angew. Chem., Int. Ed.* **2015**, *54*, 174−178. (i) Shiraishi, Y.; Tanaka, K.; Shirakawa, E.; Sugano, Y.; Ichikawa, S.; Tanaka, S.; Hirai, T. *Angew. Chem., Int. Ed.* **2013**, *52*, 8304−8308. (j) Klajn, R. *Chem. Soc. Rev.* **2014**, *43*, 148.

(6) (a) Shiraishi, Y.; Itoh, M.; Hirai, T. *Phys. Chem. Chem. Phys.* **2010**, *12*, 13737−13745. (b) Kohl-Landgraf, J.; Braun, M.; Özcoban, C.; Goncalves, D. P. N.; Heckel, A.; Wachtveitl, J. *J. Am. Chem. Soc.* **2012**, *134*, 14070−14077. (c) Chen, J.-R.; Yang, D.-Y. *Org. Lett.* **2009**, *11*, 1769−1772. (d) Shiraishi, Y.; Miyamoto, R.; Hirai, T. *Org. Lett.* **2009**, *11*, 1571−1574.

(7) (a) Doron, A.; Katz, E.; Tao, G.; Willner, I. *Langmuir* **1997**, *13*, 1783−1790. (b) Kong, L.; Wong, H. L.; Tam, A. Y. Y.; Lam, W. H.; Wu, L.; Yam, V. W. W. *ACS Appl. Mater. Interfaces* **2014**, *6*, 1550−1562. (c) Xie, X.; Mistlberger, G.; Bakker, E. *J. Am. Chem. Soc.* **2012**, *134*, 16929−16932. (d) Remon, P.; Li, S. M.; Grøtli, M.; Pischel, U.; Andreasson, J. *Chem. Commun.* **2016**, *52*, 4659−4662.

(8) (a) Kortekaas, L.; Ivashenko, O.; van Herpt, J. T.; Browne, W. R. *J. Am. Chem. Soc.* **2016**, *138*, 1301−1312. (b) Kumar, S.; van Herpt, J. T.; Gengler, R. Y. N.; Feringa, B. L.; Rudolf, P.; Chiechi, R. C. *J. Am. Chem. Soc.* **2016**, *138*, 12519−12526.

(9) (a) Wojtyk, J. T.C.; Buncel, E.; Kazmaier, P. M. *Chem. Commun.* **1998**, 1703−1704. (b) Fries, K.; Samanta, S.; Orski, S.; Locklin, J. *Chem. Commun.* **2008**, 6288−6290. (c) Guo, X.; Zhang, D.; Tao, H.; Zhu, D. *Org. Lett.* **2004**, *6*, 2491−2494. (d) Guo, Z.-Q.; Chen, W.-Q.; Duan, X.-M. *Org. Lett.* **2010**, *12*, 2202−2205.

(10) (a) Sagara, Y.; Kato, T. *Nat. Chem.* **2009**, *1*, 605−610. (b) Lee, C. K.; Davis, D. A.; White, S. R.; Moore, J. S.; Sottos, N. R.; Braun, P. V. *J. Am. Chem. Soc.* **2010**, *132*, 16107−16111. (c) Zhang, H.; Gao, F.; Cao, X.; Li, Y.; Xu, Y.; Weng, W.; Boulatov, R. *Angew. Chem., Int. Ed.* **2016**, *55*, 3040−3044.

(11) (a) Guo, X.; Zhang, D.; Zhu, D. *Adv. Mater.* **2004**, *16*, 125−130. (b) Raymo, F. M.; Alvarado, R. J.; Giordani, S.; Cejas, M. A. *J. Am. Chem. Soc.* **2003**, *125*, 2361−2364. (c) Zhu, L.; Zhu, M.-Q.; Hurst, J. K.; Li, A. D. Q. *J. Am. Chem. Soc.* **2005**, *127*, 8968−8970. (d) Giordani, S.; Raymo, F. M. *Org. Lett.* **2003**, *5*, 3559−3562. (e) Tomizaki, K.; Mihara, H. *J. Am. Chem. Soc.* **2007**, *129*, 8345−8352. (f) Nagashima, S.; Murata, M.; Nishihara, H. *Angew. Chem., Int. Ed.* **2006**, *45*, 4298−4301. (g) Raymo, F. M.; Giordani, S. *Org. Lett.* **2001**, *3*, 3475−3478.

(12) (a) Shao, N.; Zhang, Y.; Cheung, S.; Yang, R.; Chan, W.; Mo, T.; Li, K.; Liu, F. *Anal. Chem.* **2005**, *77*, 7294−7303. (b) Li, Y.; Duan, Y.; Li, J.; Zheng, J.; Yu, H.; Yang, R. *Anal. Chem.* **2012**, *84*, 4732−4738. (c) Champagne, B.; Plaquet, A.; Pozzo, J.-L.; Rodriguez, V.; Castet, F. *J. Am. Chem. Soc.* **2012**, *134*, 8101−8103.

(13) (a) Setaro, A.; Bluemmel, P.; Maity, C.; Hecht, S.; Reich, S. *Adv. Funct. Mater.* **2012**, *22*, 2425−2431. (b) Zhang, M.; Hou, X.; Wang, J.;

DOI: 10.1021/acs.joc.7b00722
J. Org. Chem. 2017, 82, 7783−7790

Tian, Y.; Fan, X.; Zhai, J.; Jiang, L. *Adv. Mater.* **2012**, *24*, 2424−2428. (c) Liu, G.; Wang, J. *Angew. Chem., Int. Ed.* **2010**, *49*, 4425−4429. (d) Silvi, S.; Arduini, A.; Pochini, A.; Secchi, A.; Tomasulo, M.; Raymo, F. M.; Baroncini, M.; Credi, A. *J. Am. Chem. Soc.* **2007**, *129*, 13378−13379. (e) Yildiz, I.; Impellizzeri, S.; Deniz, E.; McCaughan, B.; Callan, J. F.; Raymo, F. M. *J. Am. Chem. Soc.* **2011**, *133*, 871−879. (f) Byrne, R.; Diamond, D. *Nat. Mater.* **2006**, *5*, 421−424. (g) Kundu, P. K.; Samanta, D.; Leizrowice, R.; Margulis, B.; Zhao, H.; Börner, M.; Udayabhaskararao, T.; Manna, D.; Klajn, R. *Nat. Chem.* **2015**, *7*, 646−652.

(14) (a) Chen, L.; Wu, J.; Schmuck, C.; Tian, H. *Chem. Commun.* **2014**, *50*, 6443−6446. (b) Zhu, L.; Wu, W.; Zhu, M.-Q.; Han, J. J.; Hurst, J. K.; Li, A. D. Q. *J. Am. Chem. Soc.* **2007**, *129*, 3524−3526. (c) Shao, N.; Jin, J.; Wang, H.; Zheng, J.; Yang, R.; Chan, W.; Abliz, Z. *J. Am. Chem. Soc.* **2010**, *132*, 725−736. (d) Özçoban, C.; Halbritter, T.; Steinwand, S.; Herzig, L.-M.; Kohl-Landgraf, J.; Askari, N.; Groher, F.; Fürtig, B.; Richter, C.; Schwalbe, H.; Suess, B.; Wachtveitl, J.; Heckel, A. *Org. Lett.* **2015**, *17*, 1517−1520.

(15) (a) Cabrera, I.; Shvartsman, F.; Veinberg, O.; Krongauz, V. *Science* **1984**, *226*, 341−343. (b) Seki, T.; Ichimura, K.; Ando, E. *Langmuir* **1988**, *4*, 1068−1069. (c) Tachibana, H.; Yamanaka, Y.; Sakai, H.; Abe, M.; Matsumoto, M. *J. Lumin.* **2000**, *87*−*89*, 800−802. (d) Onai, Y.; Mamiya, M.; Kiyokawa, T.; Okuwa, K.; Kobayashi, M.; Shinohara, H.; Sato, H. *J. Phys. Chem.* **1993**, *97*, 9499−9505.

(16) Klajn, R. *Chem. Soc. Rev.* **2014**, *43*, 148−184.

(17) (a) Goldburt, E.; Shvartsman, F.; Krongauz, V. *Macromolecules* **1984**, *17*, 1876−1878. (b) Cabrera, I.; Krongauz, V. *Nature* **1987**, *326*, 582−585.

(18) (a) Bénard, S.; Yu, P. *Chem. Commun.* **2000**, 65−66. (b) Julia-Lopez, A.; Hernando, J.; Ruiz-Molina, D.; Gonzalez-Monje, P.; Sedo, J.; Roscini, C. *Angew. Chem., Int. Ed.* **2016**, *55*, 15044−15048. (c) Wismontski-Knittel, T.; Krongauz, V. *Macromolecules* **1985**, *18*, 2124−2126. (d) Kundu, P. K.; Olsen, G. L.; Kiss, V.; Klajn, R. *Nat. Commun.* **2014**, *5*, 3588−3596. (e) Harada, J.; Kawazoe, Y.; Ogawa, K. *Chem. Commun.* **2010**, *46*, 2593−2595.

(19) (a) Wang, M.; Vajpayee, V.; Shanmugaraju, S.; Zheng, Y.; Zhao, Z.; Kim, H.; Mukherjee, P. S.; Chi, K.-W.; Stang, P. J. *Inorg. Chem.* **2011**, *50*, 1506−1512. (b) Dong, J.; Zhou, Y.; Zhang, F.; Cui, Y. *Chem. - Eur. J.* **2014**, *20*, 6455−6461. (c) Xuan, W.; Zhang, M.; Liu, Y.; Chen, Z.; Cui, Y. *J. Am. Chem. Soc.* **2012**, *134*, 6904−6907. (d) Zhang, J.; Li, Y.; Yang, W.; Lai, S.; Zhou, C.; Liu, H.; Che, C.-M.; Li, Y. *Chem. Commun.* **2012**, *48*, 3602−3604. (e) Acharyya, K.; Mukherjee, P. S. *Chem. Commun.* **2014**, *50*, 15788−15791.

(20) (a) Murase, T.; Nishijima, Y.; Fujita, M. *J. Am. Chem. Soc.* **2012**, *134*, 162−164. (b) Zhao, C.; Sun, Q.; Hart-Cooper, W. M.; DiPasquale, A. G.; Toste, F. D.; Bergman, R. G.; Raymond, K. N. *J. Am. Chem. Soc.* **2013**, *135*, 18802−18805. (c) Zhang, Q.; Tiefenbacher, K. *J. Am. Chem. Soc.* **2013**, *135*, 16213−16219. (d) Hart-Cooper, W. M.; Clary, K. N.; Toste, F. D.; Bergman, R. G.; Raymond, K. N. *J. Am. Chem. Soc.* **2012**, *134*, 17873−17876. (e) Mondal, B.; Acharyya, K.; Howlader, P.; Mukherjee, P. S. *J. Am. Chem. Soc.* **2016**, *138*, 1709−1716. (f) Sun, J.-K.; Zhan, W.-W.; Akita, T.; Xu, Q. *J. Am. Chem. Soc.* **2015**, *137*, 7063−7066.

(21) (a) Zhang, K.; Ajami, D.; Gavette, J. V.; Rebek, J. *J. Am. Chem. Soc.* **2014**, *136*, 5264−5266. (b) Wang, W.; Wang, Y.-X.; Yang, H.-B. *Chem. Soc. Rev.* **2016**, *45*, 2656−2693. (c) Wei, P.; Yan, X.; Huang, F. *Chem. Soc. Rev.* **2015**, *44*, 815−832. (d) Zhang, M.; Yan, X.; Huang, F.; Niu, Z.; Gibson, H. W. *Acc. Chem. Res.* **2014**, *47*, 1995−2005.

(22) (a) Cougnon, F. B. L.; Sanders, J. K. M. *Acc. Chem. Res.* **2012**, *45*, 2211−2221. (b) Rowan, S. J.; Cantrill, S. J.; Cousins, G. R. L.; Sanders, J. K. M.; Stoddart, J. F. *Angew. Chem., Int. Ed.* **2002**, *41*, 898−952. (c) Reek, J. N. H.; Otto, S. *Dynamic Combinatorial Chemistry*; Wiley-VCH: Weinheim, 2010. (d) Lehn, J. M. *Chem. - Eur. J.* **1999**, *5*, 2455−2463.

(23) (a) Mitra, T.; Jelfs, K. E.; Schmidtman, M.; Ahmed, A.; Chong, S. Y. D.; Adams, J.; Cooper, A. I. *Nat. Chem.* **2013**, *5*, 276−281. (b) Jiang, S.; Jelfs, K. E.; Holden, D.; Hasell, T.; Chong, S. Y.; Haranczyk, M.; Trewin, A.; Cooper, A. I. *J. Am. Chem. Soc.* **2013**, *135*, 17818−17830. (c) Zhang, G.; Presly, O.; White, F.; Oppel, I. M.; Mastalerz, M. *Angew. Chem., Int. Ed.* **2014**, *53*, 5126−5130. (d) Ding, H.; Yang, Y.; Li, B.; Pan, F.; Zhu, G.; Zeller, M.; Yuan, D.; Wang, C. *Chem. Commun.* **2015**, *51*, 1976−1979.

(24) Blackburn, O. A.; Coe, B. J.; Helliwell, M.; Raftery, J. *Organometallics* **2012**, *31*, 5307−5320.

(25) Qi, Q.; Qian, J.; Ma, S.; Xu, B.; Zhang, S. X.; Tian, W. *Chem. - Eur. J.* **2015**, *21*, 1149−1155.

DOI: 10.1021/acs.joc.7b00722
J. Org. Chem. 2017, 82, 7783−7790